Regeneration of photon echoes with amplified photon echoes

Mohan, R. K.; Elman, U.; Tien, M.; Kröll, Stefan

Published in:
Optics Letters

1999

Regeneration of photon echoes with amplified photon echoes

R. Krishna Mohan, Ulf Elman, Mingzhen Tian, and Stefan Kröll

Department of Physics, Lund Institute of Technology (LTH), Box 118, S-221 00 Lund, Sweden

Received September 14, 1998

Photon-echo-based devices have been proposed for many applications in data storage, image processing, and optical communications. Many of these applications would benefit if the output from the photon-echo process could be used as input in a second photon-echo process. We demonstrate the generation of such secondary echoes, using the amplified output from an initial photon-echo process. The amplification is performed with a Pr:ZBLAN fiber amplifier, which gives a gain of more than 300 at 606 nm when pumped with 320 mW of power at 476 nm. © 1999 Optical Society of America

OCIS codes: 210.2860, 060.2320, 270.1670, 200.4560, 140.3510.

By use of so-called frequency-selective materials, photon-echo-based devices were shown to have a large application potential in the areas of data storage, image processing, and optical communications. Frequency selection can be performed in inhomogeneously broadened materials, in which individual atoms (molecules) in the material can be distinguished from one another because each has a slightly different absorption frequency. It is then possible to address selectively the atoms within different frequency intervals and thus to store or read a single bit of information in each interval. At liquid-helium temperatures, $>10^6$ channels can be separately addressed in certain crystals. Thus spectacular storage densities in the range of terabits per square centimeter have been envisaged.[1]

Luo *et al.* demonstrated[2] amplification of photon-echo signals in a rare-earth-doped fiber amplifier and suggested that this development could be expected to broaden the application range of photon-echo-based devices, e.g., optical bit-rate converters, routers,[3] and erasable memories. In all these applications the photon-echo output needs to be used as input for a new photon-echo process. A simple example of the applicability of echo regeneration is a scheme that has been proposed for selective erasure of photon-echo data.[4] In this scheme the data are erased by rewriting of the original data sequence into the storage material with a π-phase shift. If the data bit to be erased is read out and the resulting photon echo signal is phase shifted by 180° and sent back into the storage medium, selective erasure can be performed. This approach is intrinsically self-correcting and self-compensating for any phase, frequency, or amplitude fluctuations of the input pulses. However, since the photon-echo output intensity is generally only ~0.1% to 1% of the input intensity, it is necessary to amplify the photon-echo output pulses before sending them into the sample for the erasure process. In general, amplification of photon-echo data is important for any process in which the output of a photon-echo process should be used as input data for a later photon-echo process.

Luo *et al.*[2] reported an attractive approach for faithful amplification of photon-echo signals by use of a rare-earth-doped fiber amplifier. The photon-echo signal generated in a Pr^{3+}:Y_2SiO_5 (Pr:YSO) crystal at 606 nm (which corresponds to the $^3H_4-^1D_2$ transition) was amplified by a Pr:$ZrF_4BaF_2LaF_3AlF_3NaF$ (Pr:ZBLAN) fiber, which has a 10-nm-wide transition ($^3P_0-^3H_6$) that peaks at 605 nm. Photon-echo amplification of ~45 was achieved with a fiber with a numerical aperture (NA) of 0.4. Since the efficiency of photon-echo data storage or processing typically is 0.1–1%, a total gain in the range 100–1000 is preferable for using the echo pules as input to other photon-echo processes. A simple analysis[2] suggests that by use of a lower-NA fiber the gain could be increased by an order of magnitude, owing to a lower sensitivity to amplified spontaneous emission (ASE). In the present experiment we use a Pr:ZBLAN fiber amplifier with a NA of 0.15, which produces a gain of 300 at 606 nm, to amplify photon-echo signals from a Pr:YSO crystal. We then demonstrate that these amplified photon-echo output signals can generate new photon echoes in a secondary photon-echo process. Here we describe the features of the experiment, the characteristics of the fiber amplifier, and significant observations on echo-generation efficiency and signal-to-noise ratio when these amplified photon echoes were used as input for regeneration of new echoes. Application of this scheme for multi-data-pulse sequences is also presented.

The experimental layout for what can be termed regenerated echoes with amplified photon echoes (REAP) is given in Fig. 1. The output from an Ar-ion-laser-pumped ring dye laser was sent through an acousto-optic modulator (AOM), producing an input pulse sequence to the liquid-helium-cooled Pr:YSO crystal. The dye laser was tuned to the site 1 $^3H_4-^1D_2$ transition at 606 nm. The dye output power before the cryostat was measured to be 400 mW. The transmitted excitation pulses and the echo output sequence from the crystal were then coupled into a Pr:ZBLAN fiber (Le Verre Fluoré; $\phi = 3$ μm; $L = 30$ cm; NA, 0.15; single mode) pumped by a second Ar-ion laser at the 476-nm wavelength. The pump power coupled into the fiber was 240 mW. The 476-nm radiation and the echo signal were coupled from opposite ends of the fiber through two dichroic mirrors. The amplified output from the fiber was sent back into the crystal through a polarization rotator for echo regeneration.

0146-9592/99/010037-03$15.00/0

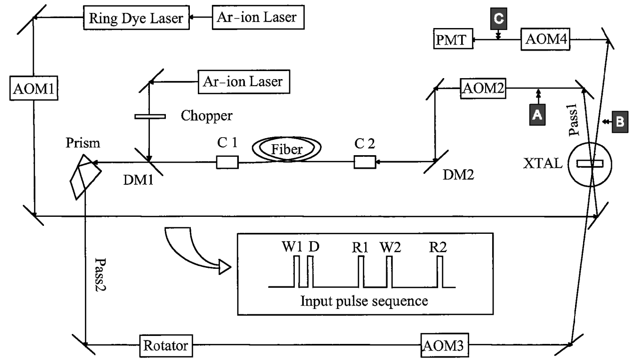

Fig. 1. Experimental setup, along with the input pulse sequence (inset): C1, C2, fiber couplers; DM1, DM2, dichroic mirrors; XTAL, crystal; D, data. See text for other definitions.

Since the echo-signal strength in the Pr:YSO crystal depends strongly on the relative orientation between the light polarization and the crystal axes, the rotator was used to compensate for any rotation of the polarization of the amplified signals that was due to the crystal and to propagation through the fiber. A five-input pulse sequence generated by AOM1 was used for the experiment (see Fig. 1, inset).

We used several other AOM's in the experimental setup to eliminate the noise and (or) background arising from scattering at the sample and ASE from the fiber. The timing sequences of the AOM's were as follows: AOM2 opened after three input pulses and closed after the fifth input pulse. Thus only the stimulated echo (that was due to the first three pulses), the fourth pulse, and the fifth pulse were allowed into the fiber for amplification. AOM3 also opened and closed during the same time, thereby allowing only the amplified pulses to enter the crystal for regeneration of a stimulated echo. This helped in avoiding unwanted ASE at 606 nm. AOM4 was used as a gate for REAP signal detection.

For the sake of clarity in nomenclature, the layout is divided into two parts, Pass1 (before the amplifier) and Pass2 (postamplifier stage). A stimulated photon-echo signal in Pass1 (point A in Fig. 1) is referred to as SPE1, a two-pulse photon echo in Pass2 (point B in Fig. 1) is referred to as TPE2, and so on. The role played by the amplifier is illustrated clearly in Fig. 2, which shows a two-pulse echo in Pass2 (TPE2) resulting from SPE1 and one additional input pulse, W2, that is incident after the SPE1 signal. In trace (a) the amplifier is off, and the photomultiplier tube (PMT) gain is ~900. In trace (b) the amplifier is on, and the PMT gain is ~20. Using these gains and the WRITE pulse height in both the traces, we calculated the amplifier gain to be ≈180. In trace (b) the REAP signal (divided by the PMT gain) is $\sim 90/20 = 4.5$ units. In trace (a) the noise level is less than 0.3 units, and the REAP signal cannot be seen. Dividing the noise level by the PMT gain (900), one can conclude that the signal strength must be smaller than that in trace (b) by a factor of 10^4 or more. [In fact, in the small-signal limit it should be a factor of $(\text{gain})^3 = 180^3 \approx 6 \times 10^6$ times smaller; thus there is nothing surprising about the fact that the signal cannot be seen.] For the case shown here the importance of a high-gain amplifier is evident, since without amplification the pulses are simply not intense enough to generate a REAP signal. Thus the usefulness of amplifying the echo output before using it as input pulses in a new photon-echo process is demonstrated.

The scheme explained here has many active and passive controls to suppress the background noise. The amplifier has a finite buildup time that was measured to be 30 μs at a pump power of 240 mW. A strong input pulse might saturate the gain of the fiber amplifier for a significant duration of time. Thus, in Pass1, AOM2 was used to allow only the photon echo, SPE1, and subsequent input pulses to go through the fiber amplifier so that they would experience the maximum gain. The amplified output from the fiber was dispersed by a Pellin–Broca prism so that the rather strong ASE at wavelengths other than 606 nm (e.g., 635 and 715 nm) was eliminated. AOM3, in Pass2, was made to function in tandem with AOM2 as described above. The 606-nm ASE (≈0.3 mW at the pump power used) was much lower than the REAP signal (≈1 mW) for a single stimulated echo used as the input. But in the case of a multi-data-pulse input the REAP signal strength can be lower than the ASE background, which would affect detection. Since AOM4, which was used in front of the PMT, opened well after the last input pulse, R2 (and AOM3 was already closed by then), all the ASE from the fiber that occurred before the REAP signal was effectively blocked.

We also extended this scheme to a multi-data-input sequence, as shown in Fig. 3, in which a 4-bit REAP sequence is generated. Trace (a) is the trace recorded by a photodiode after the crystal in Pass1. It shows one write pulse, W1, followed by four data pulses (DATA). After the first read pulse, R1, the recalled data pulses, SPE1, are shown, followed by write and read pulses for the second pass, W2 and R2, respectively. Trace (b) shows the photon-echo signal at point C (see Fig. 1), as detected by a PMT. In trace (b) we

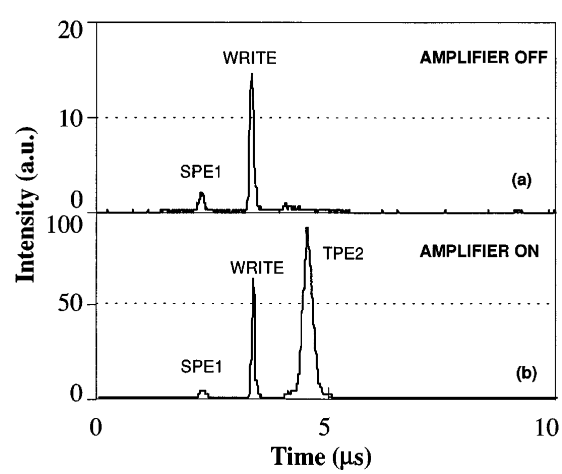

Fig. 2. Role of the amplifier in the generation of the REAP (TPE2) signal. Traces (a) and (b) are set to the same scale. The gain of the amplifier can be calculated to be ≈180.

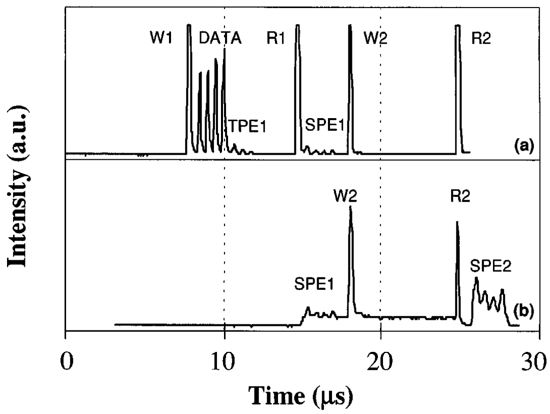

Fig. 3. (a) Pulse sequence in Pass1 (point A in Fig. 1). (b) Multi-data-pulse REAP (SPE2) signal.

first see pulses SPE1, R2, and W2 sitting on a 606-nm ASE background leaking through AOM4. We then see the recalled data from the second pass, SPE2, where the SPE1 signal is used as the input. The background and distortion in the SPE2 signal arises not from the ASE signal but from coherent saturation (see, e.g., Ref. 5).

For this process to become a technological reality with a vast application base, a deeper insight into the various mechanisms that govern the losses and gains is imperative. In addition to overall signal strength, the signal-to-noise ratio and the signal fidelity after amplification are some of the factors that need to be given serious consideration. The REAP signal strength is dependent on the losses that are due to the various active devices such as the AOM's, passive optical components, coupling into the fiber, transmission through the cryostat and crystal, and gain owing to amplification from the fiber. A simple phenomenological expression for the REAP signal strength can be written as

$$I_{\mathrm{REAP}} = \{I_{\mathrm{SPE1}}\}\{L_{\mathrm{COUP}}\}\{G_{\mathrm{AMP}}\}\{L_{\mathrm{Pass2}}\}\{\eta_{\mathrm{Pass2}}\},$$

where $I_{\mathrm{SPE1}} = \{I_{\mathrm{data}}\}\{\eta_{\mathrm{Pass1}}\}\{L_{\mathrm{Pass1}}\}$, I_x is the intensity of the corresponding pulse, L_x denotes the corresponding loss, G represents gain, and η is the echo-generation efficiency. The losses in each pass include those that are due to all the passive and active optical components. Thus if the losses and a low η could be compensated for by high gain in the amplifier, a large REAP signal could be generated with moderate input intensities.

Assuming that the loss in Pass1 is ~60% (the diffraction efficiency of AOM2 is ≈50%), that only 25% of the signal to be amplified is coupled into the fiber, and that the loss in Pass2 (prism + rotator + AOM3) is ≈70%, a gain of 150 would amplify the SPE1 strength by a factor of 5. This would be sufficient to produce a detectable REAP output. We also carried out experiments when AOM3 was removed (thus reducing the losses). With gains up to 300 being possible with this fiber amplifier, strong REAP signals were generated that could be detected even with a low-sensitivity (0.4-A/W) photodiode. An interesting outcome of the experiments was an enhancement of the echo-generation efficiency for the REAP output, by which signals as high as the transmitted echo inputs could be observed. Since the absorption in our Pr:YSO crystal is ≈80% at 606 nm, the observed signal strength corresponds to a 20% echo-generation efficiency in Pass2. This efficiency is much larger than the 0.1–1% efficiency referred to above and to our knowledge is the highest echo efficiency in solids that has been reported. However, it is known[6] that under certain conditions one can obtain very high echo-generation efficiency by tailoring the experiments carefully.

An advantage of using a fiber amplifier to amplify the echo output is that it can be conveniently integrated into a fiber-based all-optical system that could be used in telecommunications and optical computing. Photon echoes have been generated in Er-doped crystals at 1.5 μm, and these echoes have been amplified by use of commercial fiber amplifiers.[7] This approach holds strong promise for photon-echo processors in the communication-wavelength region.

In conclusion, we have demonstrated a gain of 300 at 606 nm, using a Pr:ZBLAN fiber. This fiber amplifier was used to amplify photon echoes generated in a Pr:YSO crystal. These echoes were again sent into the crystal to generate new, secondary photon echoes. We believe that the existence of techniques to generate secondary echoes by use of first-order photon echoes as input pulses will be vital for the realization of many photon-echo devices.

This research was funded by the Swedish Natural Science Research Council, the Swedish Research Council for Engineering Sciences, and the Crafoord Foundation. S. Svanberg's support is gratefully acknowledged. S. Kröll's e-mail address is stefan.kroll@fysik.lth.se.

References

1. W. R. Babbit and T. W. Mossberg, J. Opt. Soc. Am. B **11,** 1948 (1994).
2. B. Luo, U. Elman, S. Kröll, R. Paschotta, and A. Tropper, Opt. Lett. **23,** 442 (1998).
3. W. R. Babbitt and T. W. Mossberg, Opt. Lett. **20,** 910 (1995).
4. U. Elman, B. Luo, and S. Kröll, J. Opt. Soc. Am. B **13,** 1834 (1993).
5. X. A. Shen and R. Kachru, Opt. Lett. **18,** 1967 (1993).
6. M. Azadeh, C. Sjaarda Cornish, W. R. Babbitt, and L. Tsang, Phys. Rev. A **57,** 4662 (1998).
7. X. A. Shen and R. Kachru, "Amplification of photon echo signals for photon-echo-based optical storage and optical-processing devices," Proc. SPIE **3468** (to be published).